

It must be determined why the coupling of the rare-earth ion to the energy sink is weak in the chloride crystal; it must be decided whether this is caused by the high symmetry of the crystal (resulting in fewer lattice vibrations), the weak coupling of the ion to the lattice vibrations, or other factors.

ACKNOWLEDGMENTS

The author wishes to acknowledge helpful discussions with D. P. Devor and R. A. Satten. He is indebted to O. M. Stafsudd and A. F. Neminski for growing the many crystals. Technical assistance by R. J. Morrison is greatly appreciated.

Lifetime of Positrons in an Electron Gas*

J. P. CARBOTTE

Department of Physics, McMaster University, Hamilton, Ontario, Canada

(Received 14 July 1966)

New estimates of the lifetime of a positron in an electron gas are presented. The discussion is based on a modified ladder-type approximation to the electron-positron Green's function chosen so that the displaced-charge sum rule is identically satisfied. This constitutes a refinement of the simple ladder sum used by Kahana which leads to a large unphysical accumulation of charge about the positron. While this violation of the displaced-charge sum rule is, to say the least, annoying, reasons are given why it may not be very serious if one is concerned only with the computation of annihilation rates. We find, in fact, that the rates obtained in the more consistent modified ladder scheme are not very different from those quoted by Kahana although they represent a distinct improvement.

I. INTRODUCTION

WHEN a positron enters an electron gas, it faces the hazard of annihilation against one of the electrons with subsequent emission of two gamma rays. In this paper we present new estimates of the lifetime of a positron immersed in an interacting system of conduction electrons. The calculations are based on the Bethe-Goldstone approach first introduced by Kahana¹ and a modification suggested by Bergersen.² If one considers the problem of a low-energy (nonrelativistic) electron-positron pair annihilating in free space from a scattering state, one finds that the annihilation cross section is completely determined by solving the Schrödinger equation for the wave function of the pair coupled through their Coulomb field.³ In fact, the annihilation cross section depends only on the square of this wave function at $\mathbf{x}_e = \mathbf{x}_p$ where $\mathbf{x}_e(\mathbf{x}_p)$ is the electron (positron) coordinate—a result which is eminently sensible.

In the present work we are of course concerned with annihilation in the medium of all the other metallic electrons which do not participate directly in the annihilation process but are nevertheless around and capable of influencing this process in a profound way. Even in this case, however, one may well attempt as a first approximation to remain within the framework of writing down a Schrödinger-type equation for the annihilating

pair, trying at the same time to incorporate within this framework as much of the presence of the other electrons as is possible.

The first modification that seems essential is to change the bare Coulomb force to a more appropriate screened Coulomb force. This accounts for the polarization of the surrounding medium by the annihilating pair. Further, it is important to recognize that in an electron gas the Pauli exclusion principle plays an essential role. Because of the existence of an electron sea, all the plane-wave states below the Fermi surface are occupied and therefore cannot be employed in building up the electron part of the effective-pair wave function.

When these changes are made in the original Schrödinger equation it becomes a Bethe-Goldstone equation. The solution of this latter equation using a suitable effective force yields rates in fair agreement with experiment for a large number of metals. This is a striking improvement over the Sommerfeld model which fails completely to account even qualitatively for the observed rates.

The failure of the Sommerfeld model is easily understood. If one goes back to quantum electrodynamics and derives an expression for the total rate R for a many-body system of low-energy electrons and a positron, one finds that R is proportional to the *electronic density* at the *positron* averaged over all positron positions.⁴ This result is general and includes interactions. But the Sommerfeld model corresponds to ignoring all Coulomb forces so that the electronic density at the positron comes out to be the average density in the system. This

* Research supported by the National Research Council.

¹ S. Kahana, Phys. Rev. **117**, 123 (1960); **129**, 1622 (1963).

² B. Bergersen, Ph.D. thesis, Brandeis University, May 1964 (unpublished).

³ P. R. Wallace, Advan. Solid State Phys. **10** (1960).

⁴ R. A. Ferrell, Rev. Mod. Phys. **28**, 308 (1956).

is clearly a gross underestimate of the rates. After all, the conduction electrons are rather free and are coupled to the positron through an attractive Coulomb field. Under such conditions the positron should be quite effective at pulling in the electrons in its vicinity, thereby increasing the total annihilation rate. The positron Coulomb field is then an essential feature of the problem which must be taken into account in order to get reasonable results.

Intuitively one would expect the electronic density at the positron to depend most strongly on the short-range correlations between the annihilating pair. At short distances the Coulomb force is large, and treating it in Born approximation is not adequate. To get sensible rates one must certainly include, in the sense of perturbation theory, the multiple scattering of the annihilating electron off the positron. But this is precisely what the Bethe-Goldstone equation is designed to do.

The arguments presented so far are of course purely heuristic and do not represent a demonstration that the Bethe-Goldstone equation is a reasonable way of calculating rates in metals. To investigate the range of validity of this equation, it is necessary to turn to many-body perturbation theory. As mentioned previously, R depends only on the electronic density at the positron which is given by the limiting value of the electron-positron pair distribution function $g_{ep}(\mathbf{x}_e - \mathbf{x}_p)$ as $\mathbf{x}_e - \mathbf{x}_p \rightarrow 0$. This function is related trivially to a simple contraction of the electron-positron Green's function for which it is not difficult to generate a perturbation expansion. One can then show¹ that the sum of all the ladder graphs in this expansion leads directly to the Bethe-Goldstone equation. There remains of course an infinite set of Feynman diagrams unaccounted for, which represent corrections to the Bethe-Goldstone theory.

It is clearly impossible to analyze in detail all these remaining graphs, although Carbotte and Kahana⁵ were able to show that, up to *second order* in the Coulomb potential, such corrections are small. This was taken as an indication that the ladder graphs represent the dominant contribution to R . It also justifies, in some sense, the rather simple-minded Bethe-Goldstone equation approach, as an expedient way of estimating lifetimes. Such a procedure, however, is to be treated with care since in many ways its interpretation is deceptively simple. Many important questions of principle cannot be treated within this framework, in particular, self-energy effects. What we are trying to say is that while the corrections to the ladder approximation are numerically small up to *second order* they are very important in getting a complete physical picture and a proper appreciation of the precise status of the ladder approximation.⁵ We will not discuss these points further here; instead, we wish to bring up a rather disturbing feature of this approximation which was first noticed by Bergersen.

⁵ J. P. Carbotte and S. Kahana, Phys. Rev. **139**, A213 (1965).

In what follows it will again be important to keep in mind that only the value of $g_{ep}(\mathbf{x}_e - \mathbf{x}_p)$ for $\mathbf{x}_e - \mathbf{x}_p \rightarrow 0$ enters in R . On the other hand, from a knowledge of the electron-positron pair distribution function for all values of the relative coordinate $\mathbf{x}_e - \mathbf{x}_p$, one can compute the total displaced charge about the positron. To have a consistent theory one must insist that this be exactly one unit. Bergersen pointed out that in the ladder approximation, the total displaced charge can actually be considerably greater than one. For sodium it is estimated to be more than 25% greater. On this basis he argued that Kahana's rates should be reduced by a corresponding amount. We believe that this deduction is not necessarily correct. In fact the reason why the ladder approximation suggests itself at all as useful in calculating rates is precisely because this quantity depends only on the value of the pair distribution function for $\mathbf{x}_e - \mathbf{x}_p = 0$. For finite values of $\mathbf{x}_e - \mathbf{x}_p$ it cannot be expected to be as good; yet values of this function over a significant distance must certainly enter in the displaced charge calculation. In particular, Friedel oscillations occur. Thus, it would seem more likely that serious errors in $g_{ep}(\mathbf{x}_e - \mathbf{x}_p)$ for finite $\mathbf{x}_e - \mathbf{x}_p$ are responsible for most of the unphysical accumulation of charge about the positron.

We are not suggesting here that Bergersen's criticism is invalid and can be ignored. On the contrary, we believe that it is important to find an approximation scheme in which the displaced charge is exactly 1, although we do not think that this will change by large amounts the rates computed in Refs. 1. Bergersen actually indicated how this might be achieved simply by including, besides the ladder graphs, another infinite set of diagrams starting in third order in the expansion of the electron-positron Green's function. It is the aim of this paper to make a careful estimate of lifetimes within this more consistent scheme. Only a very crude estimate was attempted in Ref. 2.

The need to refine the ladder approximation is also indicated on experimental grounds. New measurements of the lifetime in aluminum by Weisberg⁶ show that the rate given in the second of Ref. 1 is considerably too large. Calculations of core annihilation in sodium by Carbotte⁷ and more recently by Carbotte and Salvadori,⁸ also lead to the same conclusion, i.e., when the core electron contribution to R is added to the conduction contribution given by Kahana one again gets too large a result as compared to Weisberg's. We might make one more point. Recently it has been found by Stewart and co-workers⁹ that there is definite evidence for a velocity-dependent annihilation rate in sodium,

⁶ J. H. Terrell, H. L. Weisberg, and S. Berko, in Proceedings of the Positron Annihilation Conference, Wayne State University, 1965 (to be published).

⁷ J. P. Carbotte, in Proceedings of the Positron Annihilation Conference, Wayne State University, 1965 (to be published).

⁸ J. P. Carbotte and A. Salvadori (to be published).

⁹ J. J. Donaghy and A. T. Stewart, American Physical Society meeting held in Philadelphia, 1964 (unpublished).

although that given in Ref. 1 seemed too weak. The present calculation gives a stronger momentum dependence.

In Sec. II the electron-positron pair distribution function is defined and related to the Green's function. The displaced charge about the positron is then studied in Born approximation and compared with the results of Langer and Vosko¹⁰ for a heavy impurity. In Sec. III the theory is extended to include the higher-order ladders. Further, the set of Feynman graphs which in our formalism corresponds to making Bergersen's so-called v_3 correction is specified. This equivalence is demonstrated by proving explicitly that the specified set indeed adds up with the ladder terms to give a total displaced charge of exactly one unit. In Sec. IV, an expression for the total annihilation rate R is derived in this "modified ladder approximation." The resulting formula agrees with that of Ref. 2. Section V is concerned mainly with the algebraic manipulations necessary to reduce the expression for R to a form that can be evaluated numerically. The numerical work is also discussed briefly. Finally, in Sec. VI we draw conclusions and compare our results with experiment.

II. DISPLACED CHARGE IN BORN APPROXIMATION

The electron-positron pair distribution function is defined as

$$g_{ep}(\mathbf{x}_e - \mathbf{x}_p) = \langle \psi^\dagger(\mathbf{x}_{el}) \psi(\mathbf{x}_{el}) \phi^\dagger(\mathbf{x}_{pl}) \phi(\mathbf{x}_{pl}) \rangle, \quad (2.1)$$

where $\psi^\dagger(\mathbf{x}_e, t)$ is the second-quantized field operator in the Heisenberg picture creating electrons while $\phi^\dagger(\mathbf{x}_p, t)$ creates positrons. The expectation value in (2.1) is to be taken in the ground state of the N electron plus positron system.¹¹ This function gives the electronic density at the position \mathbf{x}_e given that there is a positron at \mathbf{x}_p . The right-hand side of (2.1) is easily related to a contraction of the electron-positron Green's function $G_{ep}(x_1, x_2; x_1', x_2')$,

$$g_{ep}(\mathbf{x}_e - \mathbf{x}_p) = (-i)^2 G_{ep}(\mathbf{x}_{el}, \mathbf{x}_{pl}; \mathbf{x}_{el}^+, \mathbf{x}_{pl}^+), \quad (2.2)$$

where by definition

$$G_{ep}(x_1, x_2; x_1', x_2') = (-i)^2 T \langle \psi(x_1) \phi(x_2) \phi^\dagger(x_2') \psi^\dagger(x_1') \rangle. \quad (2.3)$$

The operator T in (2.3) is the Wick time-ordering operator, which orders the field operators in the expectation value according to increasing time. Notice also that the time dependence on the right-hand side in both (2.1) and (2.2) is only apparent and drops out because of translational invariance in time.

When interactions are neglected $G_{ep}(x_1, x_2; x_1', x_2')$ factors into the simple product of the free electron and

positron propagators which are denoted respectively by $G_e^0(x_1; x_1')$ and $G_p^0(x_2; x_2')$ with

$$\begin{pmatrix} G_e^0(x; x') \\ G_p^0(x; x') \end{pmatrix} = \frac{1}{V} \sum_{\mathbf{k}} e^{i\mathbf{k} \cdot (\mathbf{x} - \mathbf{x}')} \times \int \frac{d\omega}{2\pi} e^{-i\omega(t-t')} \begin{pmatrix} G_e^0(\mathbf{k}, \omega) \\ G_p^0(\mathbf{k}, \omega) \end{pmatrix}, \quad (2.4)$$

where V is the volume. The ground state of the system is specified by taking¹²

$$G_e^0(\mathbf{k}; \omega) = \frac{\theta(k - p_f)}{k^2 - \omega - i0^+} + \frac{\theta(p_f - k)}{k^2 - \omega + i0^+} \quad (2.5a)$$

and

$$G_p^0(\mathbf{k}; \omega) = \frac{\theta(k)}{k^2 - \omega - i0^+} + \frac{\theta(-k)}{-\omega + i0^+}, \quad (2.5b)$$

where $\theta(k - p_f)$ is a step function equal to 1 for k greater than the Fermi momentum p_f , and zero otherwise. The positron theta function $\theta(-k) = 0$ for $k \neq 0$ and $= 1$ for $k = 0$. In this approximation $g_{ep}(\mathbf{x}_e - \mathbf{x}_p)$ reduces trivially to

$$g_{ep}(\mathbf{x}_e - \mathbf{x}_p) = (1/V) n_e, \quad (2.6)$$

where n_e is the average electronic density in the system and the factor $1/V$ represents the positron density which we will denote by n_p . It is clear that even in the general case g_{ep} will be proportional to n_p .

The higher-order terms in the perturbation expansion for $G_{ep}(x_1, x_2; x_1', x_2')$ give the displaced charge about the positron. In particular the contribution to g_{ep} from the first-order ladder graph of Fig. 1 is

$$g_{ep}^{(1)}(\mathbf{x}_e - \mathbf{x}_p) = (-i)^2 (-i) \int d^4z d^4z' u(z; z') G_e^0(\mathbf{x}_{el}; z) \times G_p^0(\mathbf{x}_{pl}; z') G_e^0(z; \mathbf{x}_{el}^+) G_p^0(z'; \mathbf{x}_{pl}^+). \quad (2.7)$$

In (2.7), $u(z; z')$ is the dynamic effective potential in the random-phase approximation defined by the sum of the polarization bubbles. Introducing Fourier transforms for the various quantities on the right-hand side of (2.7) and carrying out the various integrations pos-

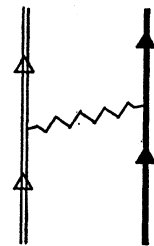


FIG. 1. The heavy solid lines represent free electron propagators, while the double light lines stand for positron propagators. The interaction line is the screened dynamic effective potential in the random-phase approximation.

¹⁰ J. S. Langer and S. H. Vosko, J. Phys. Chem. Solids 12, 196 (1959).

¹¹ The positron is assumed to be thermalized on annihilation.

¹² $\hbar^2 = 2m = 1$.

sible, one obtains

$$g_{ep}^{(1)}(\mathbf{x}_e - \mathbf{x}_p) = \frac{1}{V^2} \sum_{\mathbf{q}, \mathbf{p}} \int \frac{d\epsilon d\nu}{(2\pi)^2} u(\mathbf{q}; \nu) [e^{i\mathbf{q} \cdot (\mathbf{x}_e - \mathbf{x}_p)}] \times Q(\mathbf{q}; \nu) G_p^0(\mathbf{p}; \epsilon) G_p^0(\mathbf{p} + \mathbf{q}; \epsilon + \nu), \quad (2.8)$$

where the polarization part $Q(\mathbf{q}; \nu)$ is given by

$$Q(\mathbf{q}; \nu) = \frac{i}{V} \sum_{\mathbf{k}} \int \frac{d\omega}{(2\pi)} G_e^0(\mathbf{k} + \mathbf{q}; \omega) G_e^0(\mathbf{k}; \omega - \nu). \quad (2.9)$$

In Eq. (2.8), $u(\mathbf{q}; \nu)$ is the space-time transform of the dynamic potential and is related to the polarization part $Q(\mathbf{q}; \nu)$ by $u(\mathbf{q}; \nu) = v(\mathbf{q}) / (1 + 2v(\mathbf{q})Q(\mathbf{q}; \nu))$ with $v(\mathbf{q})$ being the Fourier transform of the Coulomb potential. Making use of Eq. (2.5b), the ϵ integration in (2.8) can be done by contour integration. Thus

$$g_{ep}^{(1)}(\mathbf{x}_e - \mathbf{x}_p) = -in_p \frac{1}{V} \sum_{\mathbf{q}} \int \frac{d\nu}{2\pi} u(\mathbf{q}; \nu) Q(\mathbf{q}; \nu) \theta(q) \times e^{i\mathbf{q} \cdot (\mathbf{x}_e - \mathbf{x}_p)} \left[\frac{1}{q^2 - \nu - i0^+} + \frac{1}{q^2 + \nu - i0^+} \right]. \quad (2.10)$$

Integrating (2.10) with respect to the relative coordinate

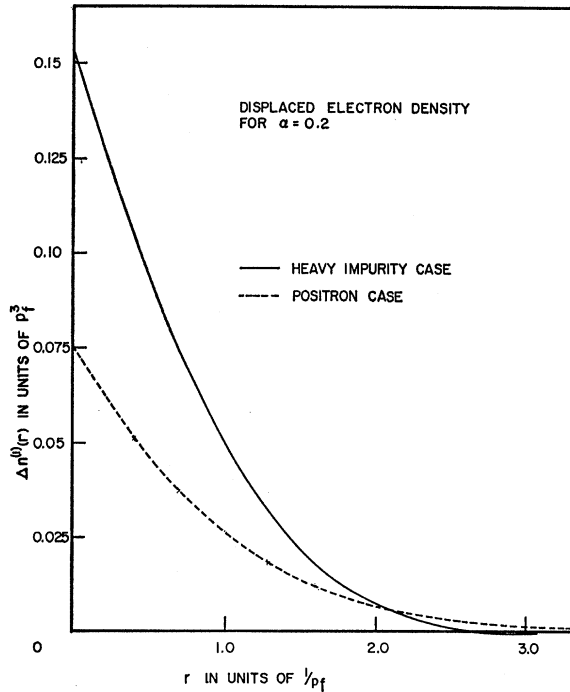


FIG. 2. Displaced electron density $\Delta n^{(1)}(r)$ (in units of p_f^3) about an impurity as a function of the distance r (in units of $1/p_f$) from the impurity site. The calculation is based on the first-order ladder graph and was carried out for an electron gas-density corresponding to $\alpha=0.2$ where $\alpha=r_s/(1.919\pi^2)$. The dashed curve is for the case of a heavy impurity while the solid curve is for a positron.

TABLE I. Shifted electron density $\Delta n^{(1)}(r) \equiv g_{ep}^{(1)}(r)/n_p$ (in units of p_f^3) as a function of the distance r (in units of $1/p_f$) away from the impurity. The calculation is based on the first-order ladder graph of Fig. 1 and was carried out for $\alpha=0.2$ where $\alpha=r_s/(1.919\pi^2)$. Results are presented both for the case of a positron and a heavy impurity.

Displacement r	Positron $\Delta n^{(1)}(r)$	Heavy-impurity $\Delta n^{(1)}(r)$
0.1	0.68380×10^{-1}	0.13909
0.4	0.51134×10^{-1}	0.10328
0.7	0.37286×10^{-1}	0.73505×10^{-1}
1.0	0.26478×10^{-1}	0.49726×10^{-1}
1.3	0.18313×10^{-1}	0.31615×10^{-1}
1.6	0.12338×10^{-1}	0.18533×10^{-1}
1.9	0.81068×10^{-2}	0.96660×10^{-2}
2.2	0.52106×10^{-2}	0.41321×10^{-2}
2.5	0.32948×10^{-2}	0.10653×10^{-2}
2.8	0.20700×10^{-2}	-0.31698×10^{-3}
3.1	0.13103×10^{-2}	-0.67027×10^{-3}
3.4	0.84930×10^{-3}	-0.49999×10^{-3}
3.7	0.57054×10^{-3}	-0.15776×10^{-3}
4.0	0.39750×10^{-3}	0.14567×10^{-3}
4.3	0.28346×10^{-3}	0.31521×10^{-3}
4.6	0.20240×10^{-3}	0.33916×10^{-3}
4.9	0.14124×10^{-3}	0.25552×10^{-3}
5.2	0.94536×10^{-4}	0.12189×10^{-3}
5.5	0.59630×10^{-4}	-0.75616×10^{-5}
5.8	0.35212×10^{-4}	-0.95991×10^{-4}
6.1	0.19727×10^{-4}	0.12889×10^{-3}
6.4	0.11185×10^{-4}	-0.11177×10^{-3}
6.7	0.73546×10^{-5}	-0.63146×10^{-4}
7.0	0.61254×10^{-5}	-0.60043×10^{-5}
7.3	0.58304×10^{-5}	0.39885×10^{-4}
7.6	0.54192×10^{-5}	0.62844×10^{-4}
7.9	0.44602×10^{-5}	0.60796×10^{-4}
8.2	0.30022×10^{-5}	0.39721×10^{-4}
8.5	0.13655×10^{-5}	0.10148×10^{-4}
8.8	-0.68460×10^{-7}	-0.16931×10^{-4}
9.1	-0.10179×10^{-5}	-0.33457×10^{-4}
9.4	-0.13798×10^{-5}	-0.36177×10^{-4}
9.7	-0.12306×10^{-5}	-0.26730×10^{-4}
10.0	-0.76902×10^{-6}	-0.10259×10^{-4}
10.3	-0.23418×10^{-6}	$+0.67833 \times 10^{-6}$

$\mathbf{x}_e - \mathbf{x}_p$ in order to get the total displaced charge about the positron amounts to projecting out the $\mathbf{q}=0$ Fourier component on the right-hand side of (2.10). This leads to a displaced charge of one unit.¹³

For arbitrary values of the electron-positron coordinate $\mathbf{x}_e - \mathbf{x}_p \equiv \mathbf{r}$, the expression (2.10) for $g_{ep}^{(1)}(\mathbf{r})$ can be reduced analytically to a double integral which must be evaluated on a computer. The numerical work is discussed in the Appendix. The computations were carried out only for $\alpha=0.2$ which corresponds roughly to sodium. The parameter $\alpha=r_s/(1.919\pi^2)$ where r_s has its usual meaning. It is the radius of a sphere in atomic units which on the average contains one conduction electron. The results for $g_{ep}^{(1)}(r)$ are shown in

¹³ A factor of 2 must be introduced for spin degeneracy. This result is independent of the use of the dynamic potential or static limit in the electron-positron interaction line of Fig. 1.

Fig. 2 for r/p_f in the range (0,3). For comparison, we have also plotted in this figure the results for a heavy impurity. The entire range (0,11) is covered in Table I.

It is clear from the figure that the electron-positron pair distribution function remains substantial over fairly large distances. Notice that the Friedel oscillations are less pronounced about the positron than about the heavy impurity and set in only further out from the impurity site. Also, the accumulated charge at the impurity is only about half as much for the positron as for the heavy charge, although it drops to zero less rapidly as we move out from the positron. In this sense, the positron does not have quite as strong an influence on the surrounding electron gas as a heavy impurity has, a result which might have been expected.

We turn now to a discussion of the second- and higher-order ladder graphs. These are known to make important contributions to the electronic density at the positron.^{1,5} Including only such graphs, however, in the calculation of the pair distribution function $g_{ep}(\mathbf{r})$ leads to a violation of the displaced charge sum rule. We will show in the next section how this difficulty can be resolved in a simple and unambiguous way.

Before leaving this section we would like to point out that the theory developed so far would for the most part apply equally well in the case of a heavy impurity center rather than a positron. The only modification necessary is to change the positron propagator $G_p(\mathbf{k}; \omega)$ given by (2.5b) to an impurity propagator $G_{imp}(\mathbf{k}; \omega)$ given by

$$G_{imp}(\mathbf{k}; \omega) = \frac{\theta(k)}{-\omega - i0^+} + \frac{\theta(-k)}{-\omega + i0^+}, \quad (2.11)$$

where we have taken the impurity mass as infinite. Making this change in (2.10), it would be replaced in an obvious notation by

$$g_{e,imp}^{(1)}(\mathbf{x}_e - \mathbf{x}_{imp}) = -in_{imp} \frac{1}{V} \sum_{\mathbf{q}} \int \frac{dv}{2\pi} -u(\mathbf{q}; v) Q(\mathbf{q}; v) \times e^{i\mathbf{q} \cdot (\mathbf{x}_e - \mathbf{x}_{imp})} \left[\frac{1}{-v - i0^+} + \frac{1}{v - i0^+} \right]. \quad (2.12)$$

The v integration in (2.12) is trivial since the principal value integral drops out and we are left only with the delta function part. Hence,

$$g_{e,imp}^{(1)}(\mathbf{x}_e - \mathbf{x}_{imp}) = n_{imp} \frac{1}{V} \sum_{\mathbf{q}} e^{i\mathbf{q} \cdot (\mathbf{x}_e - \mathbf{x}_{imp})} u(\mathbf{q}; 0) Q(\mathbf{q}; 0). \quad (2.13)$$

Passing from a summation over \mathbf{q} to an integral in (2.13) and introducing a factor of 2 for spin degeneracy, we recover the result of Langer and Vosko for a heavy impurity. Note that only the zero frequency component of the effective potential appears in (2.13). This reflects the fact that while the heavy impurity center can ab-

sorb any amount of momentum, it cannot transfer energy to the electron system.

III. EXTENSION TO HIGHER-ORDER LADDER GRAPHS

We mentioned previously that the calculation of the annihilation rate R reduces to evaluating the electron-positron pair distribution function $g_{ep}(\mathbf{r})$ in the limit $\mathbf{r} \rightarrow 0$. In fact

$$R = \lambda n(\mathbf{r}) / r = 0, \quad (3.1)$$

where $n(\mathbf{r})$ is defined by $g_{ep}(\mathbf{r}) = n_p n(\mathbf{r})$. The proportionality constant λ is equal to λ_0 / n_0 where $4\lambda_0$ is the annihilation rate in singlet positronium while n_0 is the electron density at the positron in this system. It was also pointed out that to make a reliable estimate of the short-range behavior of $g_{ep}(\mathbf{r})$ it is necessary to include in the calculation at least all the ladder graphs in the complete perturbation expansion for this function. These diagrams describe the repeated scatterings between the annihilating electron and the positron.

It is not easy to sum this restricted subset of diagrams if one insists on retaining the full dynamic effective potential $u(\mathbf{q}; v)$ in each ladder step. To make the calculation tractable, we will ignore the frequency dependence of $u(\mathbf{q}; v)$ and replace it by the static limit $u(\mathbf{q}; 0)$, a procedure which was examined in some detail and to a large extent justified in Ref. 5. Once this is done, the ladders lead directly to a Bethe-Goldstone equation. While this computational scheme is intuitively very attractive as well as simple, it does not represent a completely consistent approximation. It leads to an overaccumulation of charge about the positron which is unacceptable. The reason why this arises is simply that the first-order ladder alone exhausts the sum rule while including second- and higher-order ladders just displaces more charge.

We would like to take the point of view here, however, that this defect in the ladder approximation may not be as serious as it appears since much of the unphysical accumulation of charge about the positron is probably due to large errors in $g_{ep}(\mathbf{r})$ for finite values of \mathbf{r} rather than for $\mathbf{r} \rightarrow 0$. This idea is certainly supported by the work of Sec. II. In any case, it is still important to find a modification of the ladder approximation which does not suffer from this limitation.

This can be achieved simply by including in the calculation of $g_{ep}(\mathbf{r})$ besides the ladder graphs, another closely related infinite set of Feynman diagrams starting in third order. Before specifying these further, we would like to recall that the ladder series is summed by the integral equation,

$$G_{ep}^L(x_1, x_2; x_1', x_2') = G_e^0(x_1; x_1') G_p^0(x_2; x_2') - i \int d^4z d^4z' u(z; z') G_e^0(x_1; z) G_p^0(x_2; z') \times G_{ep}^L(z, z'; x_1', x_2'). \quad (3.2)$$

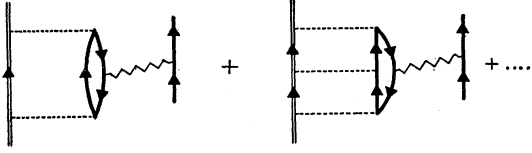


FIG. 3. Infinite set of Feynman graphs which must be included along with the second- and higher-order ladders so as to ensure that the displaced charge sum rule is satisfied. The instantaneous dashed interaction lines are to be interpreted as representing the static limit of the effective potential in the random-phase approximation.

The zeroth-order term in (3.2) and the first iterate were the subject of Sec. II. Denote by G_{ep}^{L2} the second- and higher-order iterates of (3.2) with the added provision that the static limit of the effective potential is to be used in calculating G_{ep}^{L2} . Closely related to the set of graphs for G_{ep}^{L2} is the infinite set of Fig. 3. If we denote the sum of these diagrams by G_{ep}^{LC} we can write G_{ep}^{LC} in terms of G_{ep}^{L2} , namely,

$$G_{ep}^{LC}(x_1, x_2; x_1', x_2') = (-1)i \int d^4z d^4z' G_{ep}^{L2}(z, x_2; z, x_2') \\ \times u(z; z') G_e^0(x_1; z') G_e^0(z'; x_1'). \quad (3.3)$$

Our task now is to demonstrate that when the graphs represented by (3.3) are included in the calculation of $g_{ep}(\mathbf{r})$ along with those of Eq. (3.2) the displaced charge sum rule is automatically satisfied. To show this we need only convince ourselves that $G_{ep}^{L2} + G_{ep}^{LC}$ gives a net displaced charge of zero. This can be proved as follows.

Denote the contribution of $G_{ep}^{L2} + G_{ep}^{LC}$ to the electron-positron pair distribution function by $g_{ep}^{(2)}$ and write

$$g_{ep}^{(2)}(\mathbf{r}) = \frac{1}{V} \sum_{\mathbf{q}} e^{i\mathbf{q}\cdot\mathbf{r}} g_{ep}^{(2)}(\mathbf{q}). \quad (3.4)$$

All we need to show is that $g_{ep}^{(2)}(\mathbf{q}) \rightarrow 0$ as $\mathbf{q} \rightarrow 0$. Using definition (2.2), the contribution to $g_{ep}^{(2)}(\mathbf{r})$ coming from G_{ep}^{L2} alone is

$$g_{ep}^{L2}(\mathbf{x}_e - \mathbf{x}_p) = (-1) G_{ep}^{L2}(\mathbf{x}_{el}, \mathbf{x}_{pl}; \mathbf{x}_{el}^+, \mathbf{x}_{pl}^+). \quad (3.5)$$

The right-hand side of (3.5) can of course depend only on the space variable $\mathbf{x}_e - \mathbf{x}_p$ and is independent of time. Hence it can be written in the form,

$$g_{ep}^{L2}(\mathbf{q}) = (-1) \int \frac{d\omega}{2\pi} -e^{i\omega 0^+} G_{ep}^{L2}(\mathbf{q}; \omega). \quad (3.6)$$

Further, we have from (2.2) and (3.3), after Fourier-transforming,

$$g_{ep}^{LC}(\mathbf{q}) = \int \frac{d\omega}{2\pi} -G_{ep}^{L2}(\mathbf{q}; \omega) u(\mathbf{q}; \omega) 2Q(\mathbf{q}; \omega), \quad (3.7)$$

where use was made of formula (2.9) and a factor of 2

was introduced to account for spin degeneracy. In (3.7) $g_{ep}^{LC}(\mathbf{q})$ is of course the space Fourier transform of $g_{ep}^{LC}(\mathbf{r})$. Now as $\mathbf{q} \rightarrow 0$, $u(\mathbf{q}; \omega) 2Q(\mathbf{q}; \omega) \rightarrow 1$ since $u(\mathbf{q}; \omega) = v(\mathbf{q}) / (1 + 2v(\mathbf{q})Q(\mathbf{q}; \omega))$. Hence, as $\mathbf{q} \rightarrow 0$

$$g_{ep}^{LC}(\mathbf{q}) \rightarrow \int \frac{d\omega}{2\pi} -G_{ep}^{L2}(\mathbf{q}; \omega) = -g_{ep}^{L2}(\mathbf{q}),$$

which shows that

$$g_{ep}^{(2)}(\mathbf{q}) \equiv g_{ep}^{L2}(\mathbf{q}) + g_{ep}^{LC}(\mathbf{q}) \rightarrow 0 \quad \text{as } \mathbf{q} \rightarrow 0.$$

IV. TOTAL RATE IN THE MODIFIED LADDER APPROXIMATION

The aim of this section is to derive an expression for the contribution to the total annihilation rate R coming from the sum of $g_{ep}^{L2}(\mathbf{r})$ and $g_{ep}^{LC}(\mathbf{r})$. The Fourier transform of these two quantities is given respectively by (3.6) and (3.7). From Eq. (3.1) and the relationship between $g_{ep}(\mathbf{r})$ and the displaced electron density, we get

$$R^{(2)} = \lambda \sum_{\mathbf{q}} g_{ep}^{(2)}(\mathbf{q}) \\ = -\lambda \sum_{\mathbf{q}} \int \frac{d\omega}{2\pi} -e^{i\omega 0^+} G_{ep}^{L2}(\mathbf{q}; \omega) \\ \times [1 - 2Q(\mathbf{q}; \omega) u(\mathbf{q}; \omega)], \quad (4.1)$$

where a factor of $e^{i\omega 0^+}$ was introduced in the second term of (4.1) for convenience later on in the calculation; at present it plays no role. Writing out the effective potential $u(\mathbf{q}; \omega)$ in (4.1) explicitly in terms of the bare Coulomb potential $v(\mathbf{q})$ and the R.P.A. polarization part $Q(\mathbf{q}; \omega)$, we find that

$$R^{(2)} = -\lambda \sum_{\mathbf{q}} \int \frac{d\omega}{2\pi} -e^{i\omega 0^+} G_{ep}^{L2}(\mathbf{q}; \omega) \\ \times \left(\frac{1}{1 + 2v(\mathbf{q})Q(\mathbf{q}; \omega)} \right). \quad (4.2)$$

To recover Bergersen's prescription for $R^{(2)}$, we must neglect the frequency dependence in the term $(1 + 2v(\mathbf{q}) \times Q(\mathbf{q}; \omega))$. This simplifies the calculation considerably and is in the same spirit as using the static limit for $u(\mathbf{q}; \omega)$ in second- and higher-order ladders, a procedure which is of course not rigorous but which we believe justified to a good approximation. Making this simplification yields

$$R^{(2)} = -\lambda \sum_{\mathbf{q}} L(\mathbf{q}) \int \frac{d\omega}{2\pi} -e^{i\omega 0^+} G_{ep}^{L2}(\mathbf{q}; \omega), \quad (4.3)$$

with

$$L(\mathbf{q}) = 1 / [1 + 2v(\mathbf{q})Q(\mathbf{q}; 0)]. \quad (4.4)$$

Equation (4.3) can be reduced further using a technique very similar to that used in the derivation of a theory of positron annihilation in real metals by the present

author.¹⁴ It does not seem worth while to repeat the details here. We will confine ourselves to the main points. First, instead of calculating

$$\int \frac{d\omega}{2\pi} e^{i\omega 0^+} G_{ep} L^2(\mathbf{q}; \omega)$$

directly, it is more convenient to include the first two terms in the ladder sum as well and to calculate

$$\int \frac{d\omega}{2\pi} e^{i\omega 0^+} G_{ep} L(\mathbf{q}; \omega) \equiv I^L(\mathbf{q}).$$

The extra terms will be excluded later.

To evaluate $I^L(\mathbf{q})$, we introduce as in Ref. 14 an intermediate amplitude Ω^L according to the prescription,

$$G_{ep} L(\mathbf{x}_{el}, \mathbf{x}_{pl}; \mathbf{x}_{el}^+, \mathbf{x}_{pl}^+) = \int d^4z d^3z' \Omega^L(\mathbf{x}_{el}, \mathbf{x}_{pl}; z, z') \times G_e^0(z; \mathbf{x}_{el}^+) G_p^0(z'; \mathbf{x}_{pl}^+). \quad (4.5)$$

This definition is clearly consistent with the structure of the integral equation (3.2) for $G_{ep} L(x_1, x_2; x_1', x_2')$. We now rewrite $I^L(\mathbf{q})$ in terms of Ω^L , whence

$$-\sum_{\mathbf{q}} L(\mathbf{q}) I^L(\mathbf{q}) = -\frac{1}{V} \sum_{\substack{\mathbf{m}\mathbf{n} \\ \mathbf{m}\mathbf{n}'}} L(\mathbf{m}-\mathbf{m}') \int \frac{d\omega}{2\pi} e^{i\omega 0^+} \times [i\Omega_{\mathbf{m},\mathbf{n}; \mathbf{m}',\mathbf{n}'} L(\omega) (\not{p}_{\mathbf{m}',\mathbf{n}'}^+ + \not{p}_{\mathbf{m}',\mathbf{n}'}^-) (\omega)], \quad (4.6)$$

where

$$\not{p}_{\mathbf{m},\mathbf{n}}^+(\omega) = \frac{\theta(m-p_f)\theta(n)}{m^2+n^2-\omega-i0^+}, \quad (4.7)$$

$$\not{p}_{\mathbf{m},\mathbf{n}}^-(\omega) = \frac{-\theta(p_f-m)\theta(-n)}{m^2-\omega+i0^+},$$

and where $\Omega_{\mathbf{m},\mathbf{n}; \mathbf{m}',\mathbf{n}'} L(\omega)$ is the space-time Fourier transform of the amplitude $\Omega^L(x, x'; z, z')$ which by its definition (4.5) is needed only for $t_x = t_{x'}$ and $t_z = t_{z'}$ thus can be defined only on $(t_x - t_z)$.

At this point we refer the reader to the Appendix of Ref. 14 where it is shown how the ω integration in (4.6) can be performed, with the result that

$$-\sum_{\mathbf{q}} L(\mathbf{q}) I^L(\mathbf{q}) = \frac{-i}{V} \sum_{\substack{\mathbf{m}\mathbf{n} \\ \mathbf{m}\mathbf{n}'}} L(\mathbf{m}-\mathbf{m}') \times \sum_{\substack{\mathbf{p} \\ |\mathbf{p}| < p_f}} i\Omega_{\mathbf{m},\mathbf{n}; \mathbf{p},0^0}(\not{p}^2) \Omega_{\mathbf{m}',\mathbf{n}'; \mathbf{p},0^0}(\not{p}^2) = \frac{1}{V} \sum_{\mathbf{q}} \theta(p_f - p) \sum_{\mathbf{m}} L(\mathbf{m}-\mathbf{m}') \left(\sum_{\mathbf{n}} \Omega_{\mathbf{m},\mathbf{n}; \mathbf{p},0^0}(\not{p}^2) \right) \left(\sum_{\mathbf{n}'} \Omega_{\mathbf{m}',\mathbf{n}'; \mathbf{p},0^0}(\not{p}^2) \right)^*. \quad (4.8)$$

The amplitude $\Omega_{\mathbf{m},\mathbf{n}; \mathbf{m}',\mathbf{n}'}^0(E)$ satisfies the equation

$$\Omega_{\mathbf{m},\mathbf{n}; \mathbf{m}',\mathbf{n}'}^0(E) = \delta_{\mathbf{m},\mathbf{m}'} \delta_{\mathbf{n},\mathbf{n}'} + \not{p}_{\mathbf{m},\mathbf{n}}^+(E) \frac{1}{V} \sum_{\mathbf{q}} u(\mathbf{q}; 0) \Omega_{\mathbf{m}-\mathbf{q},\mathbf{n}+\mathbf{q}; \mathbf{m}',\mathbf{n}'}^0(E). \quad (4.9)$$

From the structure of Eq. (4.9) we conclude that $\mathbf{m} + \mathbf{n} = \mathbf{m}' + \mathbf{n}'$. Incorporating this symmetry into (4.8) gives

$$\frac{1}{V} \sum_{\mathbf{q}} \theta(p_f - p) \sum_{\mathbf{m},\mathbf{m}'} L(\mathbf{m}-\mathbf{m}') \times \Omega_{\mathbf{m},\mathbf{p}-\mathbf{m}; \mathbf{p},0^0}(\not{p}^2) \Omega_{\mathbf{m}',\mathbf{p}-\mathbf{m}'; \mathbf{p},0^0}(\not{p}^2). \quad (4.10)$$

Now recall that $R^{(2)}$ is determined by $G_{ep} L^2$ rather than $G_{ep} L$. Hence dropping the zeroth- and first-order contributions in (4.10), we find from (4.3) that

$$R^{(2)} = \frac{\lambda}{V} \sum_{\mathbf{q}} \theta(p_f - p) \left[\sum_{\mathbf{m}} L(\mathbf{m}-\mathbf{p}) \chi_p^{(2)}(\mathbf{m}) + \sum_{\mathbf{m}'} L(\mathbf{p}-\mathbf{m}') \chi_p^{(2)}(\mathbf{m}') + \sum_{\mathbf{m},\mathbf{m}'} \chi_p(\mathbf{m}) L(\mathbf{m}-\mathbf{m}') \chi_p(\mathbf{m}') \right], \quad (4.11)$$

where the amplitude $\chi_p(\mathbf{m})$ satisfies the equation

$$\chi_p(\mathbf{m}) = \frac{\theta(m-p_f)}{m^2 + (\mathbf{p}-\mathbf{m})^2 - p^2} \left[\frac{1}{V} u(\mathbf{m}-\mathbf{p}; 0) + \frac{1}{V} \sum_{\mathbf{q}} u(\mathbf{q}; 0) \chi_p(\mathbf{m}-\mathbf{q}) \right], \quad (4.12)$$

and $\chi_p^{(2)} \mathbf{m}$ stands for the second- and higher-order parts of the solution of (4.12). Equation (4.11) agrees with the prescription given by Bergersen which he derived using quite a different formalism. Equation (4.12) is the Bethe-Goldstone equation of Ref. 1. We now want to evaluate (4.11) numerically. This is discussed in Sec. V.

V. ALGEBRAIC REDUCTION AND NUMERICAL EVALUATION OF $R^{(2)}$

To evaluate (4.11) numerically, it is first necessary to reduce it to a more convenient form. First taking the limit of infinite volume expression, (4.11) and Eq. (4.12) can be replaced by

$$R^{(2)} = \lambda \frac{2}{(2\pi)^3} \int_{|\mathbf{p}| < p_f} d^3\mathbf{p} \left[2 \int d^3\mathbf{m} L(\mathbf{m}-\mathbf{p}) \chi_p^{(2)}(\mathbf{m}) + \int d^3\mathbf{m} d^3\mathbf{m}' \chi_p(\mathbf{m}) L(\mathbf{m}-\mathbf{m}') \chi_p(\mathbf{m}') \right] \quad (5.1)$$

lations described particularly in the Appendix of this paper are actually more complicated than is necessary here because they include the added complication of a crystal potential.

¹⁴ J. P. Carbotte, Phys. Rev. 144, 309 (1966). The manipu-

and

$$\chi_p(\mathbf{m}) = \frac{\theta(m-p_f)}{m^2 + (\mathbf{p}-\mathbf{m})^2 - p^2} \left[\frac{u(\mathbf{m}-\mathbf{p}; 0)}{(2\pi)^3} + \int \frac{d^3\mathbf{q}}{(2\pi)^3} u(\mathbf{m}-\mathbf{q}; 0) \chi_p(\mathbf{q}) \right]. \quad (5.2)$$

Note that in (5.1) we have introduced a factor of 2 to account for spin degeneracy. Next, measuring all momenta in units of the Fermi momentum p_f and introducing the parameter $\alpha = r_s / (1.919\pi^2)$ as well as the Sommerfeld rate

$$R^0 = \lambda \frac{2}{(2\pi)^3} \frac{4\pi}{3} \frac{1}{k_F^3} \cong 12.0 / r_s^3 \times 10^9 \text{ sec}^{-1} \text{ leads to}$$

$$R^{(2)} = \frac{3}{4\pi} R^0 \int_{|\mathbf{p}| < p_f} d^3\mathbf{p} \left[2 \int d^3\mathbf{m} \mathcal{L}(\mathbf{m}-\mathbf{p}) \bar{\chi}_p^{(2)}(\mathbf{m}) + \int d^3\mathbf{m} d^3\mathbf{m}' \bar{\chi}_p(\mathbf{m}) \mathcal{L}(\mathbf{m}-\mathbf{m}') \bar{\chi}_p(\mathbf{m}') \right], \quad (5.3)$$

where

$$\mathcal{L}(\mathbf{q}) = q^2 / \left\{ q^2 + \alpha 2\pi \left[1 - \frac{1}{2q} \left(1 - \frac{1}{4}q^2 \right) \ln \left(\frac{q-2}{q+2} \right)^2 \right] \right\} \quad (5.4)$$

and

$$\bar{\chi}_p(\mathbf{m}) = \frac{1}{m^2 + (\mathbf{p}-\mathbf{m})^2 - p^2} \left[U(\mathbf{m}-\mathbf{p}) + \int d^3\mathbf{q} U(\mathbf{m}-\mathbf{q}) \bar{\chi}_p(\mathbf{q}) \right] \quad \text{for } m > 1$$

$$= 0 \quad \text{for } m < 1 \quad (5.5)$$

with

$$U(\mathbf{q}) = \alpha / [q^2 + \alpha Q^0(q)],$$

$$Q^0(q) = 2\pi \left[1 - \frac{1}{2q} \left(1 - \frac{1}{4}q^2 \right) \ln \left(\frac{q-2}{q+2} \right)^2 \right].$$

Our first task is to evaluate the amplitude $\bar{\chi}_p(\mathbf{m})$. We first notice that for $\mathbf{p}=0$, i.e., for an electron at the center of the Fermi sea, $\bar{\chi}_0(\mathbf{m})$ can depend only on the modules of \mathbf{m} . The equation is then one dimensional and can be solved numerically with relative ease. For finite values of \mathbf{p} , the situation is not as simple; however, following Kahana we will in this case average both sides of (5.5) over the angles of \mathbf{p} , a procedure which yields a tractable integral equation, namely, ($m > 1$)

$$\hat{\chi}_p(m) = \int_{|m-p|}^{m+p} \frac{U(\rho)}{m^2 + \rho^2 - p^2} \frac{\rho d\rho}{2m\rho} + \frac{\pi}{2m^2 p} \ln \left(\frac{m^2 + (m+p)^2 - p^2}{m^2 + (m-p)^2 - p^2} \right) \times \int_1^\infty q dq \bar{\chi}_p(q) \int_{|m-q|}^{m+q} U(\rho) \rho d\rho. \quad (5.6)$$

Equation (5.6) was solved using a 41-point grid in the interval (1 to 37) which is substantially finer than that used in Ref. 1. This leads to a set of inhomogeneous linear equations which were solved by successive elimination. The computations were carried out for electron-gas densities corresponding to aluminum ($\alpha=0.109$) as well as $\alpha=0.15$ and $\alpha=0.25$. In each case, (5.6) was evaluated for five values of p , namely, $p=0.1, 0.3, 0.5, 0.7, 0.9$.

In the approximation when $\bar{\chi}_p(\mathbf{m})$ is replaced by the spherical average $\hat{\chi}_p(m)$, Eq. (5.3) reduces to

$$R^{(2)} = 3R^0 \int_0^1 p^2 dp \epsilon^{(2)}(p), \quad (5.7)$$

where $\epsilon^{(2)}(p)$ is called the enhancement factor (in second and higher order) and is given by

$$\epsilon^{(2)}(p) = 8\pi \int_1^\infty m dm \hat{\chi}_p^{(2)}(m) \frac{1}{p} \int_{m-p}^{m+p} \frac{\rho d\rho}{2} \frac{\rho^2}{\rho^2 + \alpha Q^0(\rho)} + 16\pi \int_1^\infty m dm \hat{\chi}_p(m) \int_1^\infty m' dm' \hat{\chi}_p(m') \times \int_{|m-m'|}^{m+m'} \frac{\rho d\rho}{2} \frac{\rho^2}{\rho^2 + \alpha Q^0(\rho)}. \quad (5.8)$$

For a given electron gas density and a particular p , the numerical solution for $\hat{\chi}_p(m)$ and $\hat{\chi}_p^{(2)}(m)$ were read into the computer for all values of m which then proceeded to evaluate the necessary double and triple integral in (5.8). We might point out in passing that $\hat{\chi}_p^{(2)}(m)$ is, of course, $\hat{\chi}_p(m)$ minus the first term on the right-hand side of (5.6) which was also calculated in the course of the solution of this equation. In this way, we arrived at the second order enhancement factors given in Table II. From these enhancement factors, it is a simple matter to evaluate $R^{(2)}$ according to (5.7). To get a final result we must, of course, add on to $R^{(2)}$ the contribution to the total annihilation rate from the Sommerfeld term and the first-order ladder. These corrections can be handled by simply adding on to $\epsilon^{(2)}(p)$ before carrying out the p integration indicated in (5.7), 1 for the Sommerfeld term and $\epsilon^{(1)}(p)$ for the first-order ladder, where, at

TABLE II. Values of the enhancement factor $\epsilon^{(2)}(p)$ as a function of momentum p for three values of α , i.e., electron-gas densities. The enhancement factor $\epsilon^{(2)}(p)$ is a measure of the contribution to the total annihilation rate coming from the second- and higher-order ladders as well as the infinite set of diagrams given in Fig. 3. This latter set must be included so as to ensure that the displaced charge sum rule is not violated.

$\alpha =$	$p=0.1$	$p=0.3$	$p=0.5$	$p=0.7$	$p=0.9$
0.109	1.1456	1.1819	1.2615	1.4065	1.7031
0.15	2.4650	2.5409	2.7075	3.0128	3.6483
0.25	12.1067	12.5619	13.5802	15.5417	20.0650

TABLE III. Values of the total enhancement factor (in the modified ladder approximation) $\epsilon(p)$ as a function of momentum p for various values of α .

$\alpha =$	$p=0.1$	$p=0.3$	$p=0.5$	$p=0.7$	$p=0.9$
0.109	3.2040	3.2549	3.3653	3.5627	3.9541
0.15	4.8402	4.9321	5.1321	5.4934	6.2301
0.25	15.1791	15.6527	16.7084	18.7315	23.3660

least in the static approximation,

$$\epsilon^{(1)}(p) = \int_1^\infty m dm 4\pi \int_{m-p}^{m+p} \frac{\rho d\rho}{p} \frac{U(\rho)}{m^2 + \rho^2 - p^2}. \quad (5.9)$$

When this is done we get a composite result for $\epsilon(p) = 1 + \epsilon^{(1)}(p) + \epsilon^{(2)}(p)$, as tabulated in Table III. Finally the total annihilation rate in the modified ladder approximation is related to $\epsilon(p)$ by

$$R = 3R^0 \int_0^1 p^2 dp \epsilon(p).$$

This last integral could be done numerically. Instead we preferred to follow Kahana and write $\epsilon(p)$ in the form $a + bp^2 + cp^4$. The parameters a, b, c can be determined from the data of Table III and are given in Table IV. The final p integration is now trivial. The total annihilation rate R as a function of electron gas density is plotted in Fig. 4.

VI. DISCUSSION AND CONCLUSION

We have studied in some detail the displaced electron density about a positron in the high-density limit which

TABLE IV. Annihilation rates in units of $R^0 \cong 12.0/r_s^3 \times 10^9 \text{ sec}^{-1}$ obtained from the momentum-dependent enhancement factor $\epsilon(p) = a + bp^2 + cp^4$.

$\alpha =$	a	b	c	R in units of R^0
0.109	3.1983	0.56537	0.41049	3.713
0.15	4.8303	0.97833	0.91520	5.810
0.25	15.1326	4.5793	6.8955	20.835

is obtained when only the first-order ladder graph is included in the calculation. The displaced charge sum rule is automatically satisfied in this approximation. This sum rule incorporates the consistency requirement that the positron charge be neutralized by the shift of exactly one unit of electronic charge.

It is found that the displaced electron density is not as peaked about the positron as in the case of a heavy charge impurity. Also the Friedel oscillations are somewhat weaker and set in only at larger distances from the impurity site. Thus, the positron does not have as profound an influence on its surroundings as a heavy impurity: a result which is not unexpected. More important to the present discussion is the fact that the electron positron pair distribution function remains significant over quite large distances. Thus, values of this function away from the impurity center, as well as close in, are important in a computation of the total displaced charge.

When one accounts for the higher-order ladder graphs (as is necessary to extend the theory to lower electron gas densities), the displaced charge sum rule is no longer satisfied. It is, in fact, violated quite severely and hence the calculation is left open to serious criticism,

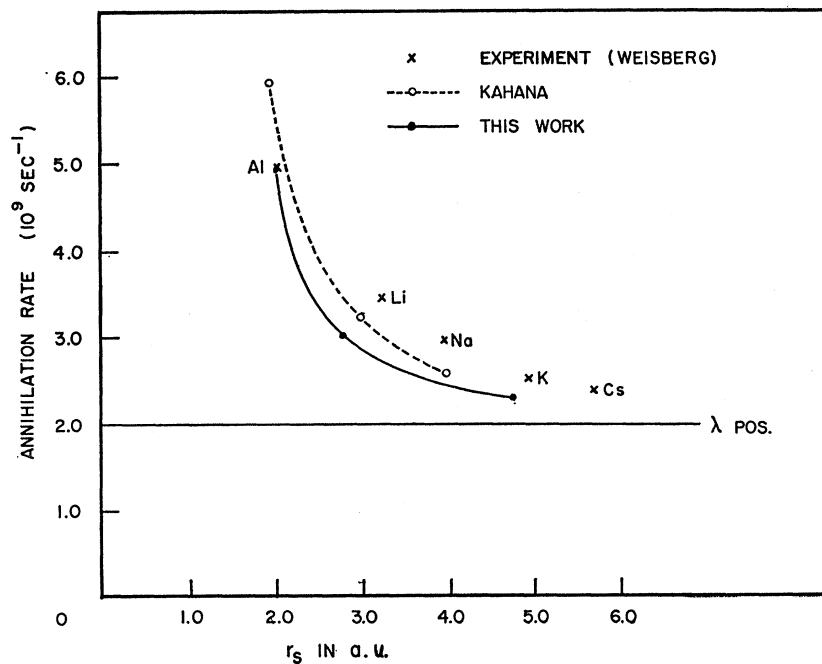


FIG. 4. The total annihilation rate as a function of electron gas density in the modified ladder approximation. The results of Kahana's original calculation are also plotted for comparison as well as Weisberg's experimental results. Except for the curve labeled "this work," this figure is the same as Fig. 4 of Ref. 6.

even though the rates obtained in this way are in good agreement with experiment. On the other hand, one is somewhat reassured when it is realized that the ladder approximation to $g_{ep}(\mathbf{x}_e - \mathbf{x}_p)$ is best for $\mathbf{x}_e - \mathbf{x}_p \rightarrow 0$ which determines R while the displaced charge sum rule is dependent on $g_{ep}(\mathbf{x}_e - \mathbf{x}_p)$ for all values of the relative coordinate. Thus, Bergersen's criticism is, to our mind, not as serious as he thought. In any case, it is possible to fix up the ladder approximation simply by including in the calculation of $g_{ep}(\mathbf{x}_e - \mathbf{x}_p)$ the further infinite subset of Feynman graphs in the expansion of the electron positron Green's function shown in Fig. 3. This leads to a modified ladder approximation for which the displaced charge is exactly one.

The main object of this paper was to make a computation of lifetimes for various electron gas densities, in this more consistent framework. We might point out that this involves rather lengthy calculations, although it is still a very much easier task than computing the displaced charge about the positron for the entire range (0 to ∞). Such a calculation would, of course, be interesting from a theoretical viewpoint, but it seems to us unjustified at present since this function is not measured directly in lifetime experiments which depend only on $g_{ep}(0)$. It seems to us, however, that a similar calculation in the case of a heavy impurity is important. The usual theory of the displaced charge about a fixed impurity center, as given for instance in Ref. 10, is really a high-density theory. The modified ladder approximation appears to be a convenient way of extending these results to lower densities. It would certainly give important corrections for values of r_s found in real metals. A paper on this subject will follow.

The total annihilation rate R as a function of electron gas density obtained in this work is plotted in Fig. 4. Our suspicion that the violation of the displaced charge sum rule in the ladder approximation is not terribly important for the calculation of R is more or less born out, although there are important differences between the results of the ladder and modified ladder schemes. The rate in aluminum in particular is substantially reduced over that quoted by Kahana. In general, the agreement with experiment is improved. In this regard the following point is worth making.

As can be seen from Table IV the total enhancement factor for $\alpha = 0.25$ comes out to be about 21 which means that the electron density at the positron is in this case 21 times larger than the average electronic density in the system. Considering that to get R one must further multiply this factor by R^0 (the Sommerfeld rate) which varies like $1/r_s^3$, it is remarkable that our curve tends so well towards λ_{pos} as r_s becomes large.

The theoretical curve does not pass through the experimental points of Weisberg which are also plotted in Fig. 4. This is to be expected since lattice effects in the conduction electron gas must certainly have an influence on the rates. That such corrections can be important is

clear from the angular correlation experiments on lithium and in particular beryllium¹⁵ where distinct anisotropies are observed in the two photon counting rate. Further, some core annihilation must certainly occur as can be seen from the results in sodium. Besides the inverted parabola type distribution with cutoff at the Fermi momentum p_f expected from the conduction electrons, one finds broad and rather long tails extending well beyond p_f which to a large extent must come from core annihilation. Thus one should at least add on to our electron gas results (which treat only the conduction electrons) a core contribution.

It is interesting in this respect that the experimental points generally fall above the theoretical curve of Fig. 4. This observation, however, should not be given too much weight since metals with large cores are also those where the Bloch states for the conduction electrons deviate seriously from plane waves. Using a plane wave theory for the conduction electrons is suspect in this case. Lattice corrections to our electron gas theory may well have the opposite effect to core annihilation, i.e., reducing the rates quoted here for the conduction electrons. This question is as yet unsettled. One would think, however, that the situation in sodium should be clear cut. An electron gas theory is certainly respectable for sodium. Also, there now exists a reasonably reliable estimate of core annihilation⁸ for this metal.

If one assigns all the discrepancy between theory and experiment indicated in Fig. 4 to core annihilation, one concludes that this contribution should be about $0.64 \times 10^9 \text{ sec}^{-1}$ or about $3.3R^0$. The calculations of Ref. 8 give $3.5R^0$. This agreement is certainly very good. We need to point out, however, that if a comparison is made with the more detailed information available from angular-correlation data there still remains some disagreement with experiment. In particular, the experiments seem to pick up less events in the "tails" than the present theory predicts.

In conclusion, the "modified ladder approximation" gives better agreement with experiment than the theory of Ref. 1, although the much simpler ladder approximation used there certainly picks up the dominant contributions to R . Thus this simpler approximation should be adequate in generalizing the present theory to include lattice effects as was done in Ref. 14. The further refinements discussed here should represent only minor corrections.

ACKNOWLEDGMENTS

The author would like to acknowledge a number of discussions with Ed Woll, Jr. The manuscript for this paper was prepared while the author was a visitor at the Physics Division of the Aspen Institute for Humanistic Studies. It is a pleasure to thank the Physics Division for its hospitality.

¹⁵ S. Berko, Phys. Rev. **128**, 2166 (1962).

APPENDIX

In this Appendix we want to reduce and evaluate numerically the electron-positron pair distribution function $g_{ep}^{(1)}(\mathbf{r})$ as given by Eq. (2.10). It is convenient to first go to the limit of infinite volume so that momentum sums go into integrals. Introducing a factor of 2 for spin degeneracy gives

$$\Delta n^{(1)}(\mathbf{r}) = -i \frac{2}{(2\pi)^3} \int d^3q \int \frac{dv}{2\pi} u(\mathbf{q}; v) \times Q(\mathbf{q}; v) e^{i\mathbf{q}\cdot\mathbf{r}} \left[\frac{2}{q^2 - v - i0^+} \right], \quad (\text{A1})$$

where we have defined $\Delta n^{(1)}(\mathbf{r}) \equiv g_{ep}^{(1)}(\mathbf{r})/n_p$ and used the fact that $Q(-\mathbf{q}; -v) = Q(\mathbf{q}; v)$, a property which is easily verified from Eq. (2.9). Further, since the effective potential $u(\mathbf{q}; v)$ and the polarization part $Q(\mathbf{q}; v)$ depend only on the magnitude of the vector \mathbf{q} , the angular part of the \mathbf{q} integration in (A1) can be done easily by choosing the z axis of integration along the direction of \mathbf{r} . This yields

$$\Delta n^{(1)}(\mathbf{r}) = -i \frac{2}{(2\pi)^3} \int_0^\infty q^2 dq \frac{4\pi \sin(qr)}{qr} \times \int_{-\infty}^{+\infty} \frac{dv}{2\pi} u(\mathbf{q}; v) Q(\mathbf{q}; v) \frac{2}{q^2 - v - i0^+}. \quad (\text{A2})$$

Next we change the v integration in (A2) from the real to the imaginary axis. Since all the singularities of the integrand in (A2) as a function of a complex variable v are either in the second or fourth quadrants,¹⁶ this

¹⁶ For a detail discussion of the singularities of $u(q;v)$ and $Q(q;v)$ see D. F. Dubois, Ann. Phys. (N. Y.) **1**, 174 (1959).

switch can be effected without any corrections being necessary. We get

$$\Delta n^{(1)}(r) = \frac{2}{(2\pi)^3} \int_0^\infty q dq \frac{\sin(qr)}{r} 4\pi \int_0^\infty \frac{dv}{2\pi} \times u(\mathbf{q}; iv) Q(\mathbf{q}; iv) \frac{4q^2}{q^4 + v^2}, \quad (\text{A3})$$

where we have further restricted the v integration to the interval $(0, \infty)$. Finally, making the transformation $q \rightarrow qp_f$ and $v \rightarrow vqp_f^2$ leads to

$$\Delta n^{(1)}(r) = p_f^3 \int_0^\infty \frac{q^2 dq \sin(qr)}{\pi^3 r} \times \int_0^\infty \frac{d\omega}{q^2 + \omega^2} \frac{\alpha \bar{Q}(q; \omega)}{q^2 \times \alpha \bar{Q}(q; \omega)}, \quad (\text{A4})$$

with

$$\bar{Q}(q; \omega) = 2\pi \left\{ 1 - \frac{1}{2q} (1 - 0.25 \times [q^2 - \omega^2]) \ln \left(\frac{\omega^2 + (q-2)^2}{\omega^2 + (q+2)^2} \right) - \frac{\omega}{2} \left[\tan^{-1} \left(\frac{2-q}{\omega} \right) + \tan^{-1} \left(\frac{2+q}{\omega} \right) \right] \right\}. \quad (\text{A5})$$

The parameter $\alpha = r_s / (1.919\pi^2)$. Integral (A4) was evaluated numerically only for $\alpha = 0.2$. The ω integration was done first using Simpson's rule with a 121-point mesh. This yields a function of q . This second integration was then carried out using a 401-point mesh with Filon's method.